Chalcone Derivatives Antagonize Interactions between the Human Oncoprotein MDM2 and p53[†]

Raphael Stoll,[‡] Christian Renner,[‡] Silke Hansen,[§] Stefan Palme,[§] Christian Klein,[§] Anja Belling,[‡] Wojciech Zeslawski,[‡] Mariusz Kamionka,[‡] Till Rehm,[‡] Peter Mühlhahn,[‡] Ralf Schumacher,[§] Friederike Hesse,[§] Brigitte Kaluza,[§] Wolfgang Voelter,[#] Richard A. Engh,[‡,§] and Tad A. Holak*[,‡]

Max Planck Institute of Biochemistry, D-82152 Martinsried, Germany, Roche Diagnostics GmbH, Pharmaceutical Research, D-82372 Penzberg, Germany, and Tübingen University, Department of Physical Biochemistry, Institute of Physiological Chemistry, D-72076 Tübingen, Germany

Received April 24, 2000; Revised Manuscript Received October 2, 2000

ABSTRACT: The oncoprotein MDM2 inhibits the tumor suppressor protein p53 by binding to the p53 transactivation domain. The p53 gene is inactivated in many human tumors either by mutations or by binding to oncogenic proteins. In some tumors, such as soft tissue sarcomas, overexpression of MDM2 inactivates an otherwise intact p53, disabling the genome integrity checkpoint and allowing cell cycle progression of defective cells. Disruption of the MDM2/p53 interaction leads to increased p53 levels and restored p53 transcriptional activity, indicating restoration of the genome integrity check and therapeutic potential for MDM2/p53 binding antagonists. Here, we show by multidimensional NMR spectroscopy that chalcones (1,3-diphenyl-2-propen-1-ones) are MDM2 inhibitors that bind to a subsite of the p53 binding cleft of human MDM2. Biochemical experiments showed that these compounds can disrupt the MDM2/p53 protein complex, releasing p53 from both the p53/MDM2 and DNA-bound p53/MDM2 complexes. These results thus offer a starting basis for structure-based drug design of cancer therapeutics.

Amplification of the *MDM2* gene is observed in a variety of human tumors (*1*, *2*). MDM2 is an oncogene product that binds to the transactivation domain of the p53 tumor suppressor protein (*3*−*6*). By binding to p53, MDM2 inhibits the ability of p53 to activate transcription (*7*) and promotes the rapid degradation of p53 (*8*, *9*). Increasing MDM2 levels thus raises the signal threshold necessary for p53-induced apoptosis (*7*−*11*) and retards the rate of the p53-induced expression of the cell cycle inhibitor p21 (*10*, *12*). Studies comparing MDM2 overexpression and p53 mutation concluded that these are mutually exclusive events, supporting the notion that the primary impact of MDM2 amplification in cancer cells is the inactivation of the resident wild-type p53 (*1*, *2*, *7*). It has been shown recently that a peptide homologue of p53 is sufficient to induce p53-dependent cell death in cells overexpressing MDM2 (*13*). This result provides clear evidence that disruption of the p53/MDM2 complex might be effective in cancer therapy.

Chalcone derivatives (compounds derived from 1,3-diphenyl-2-propen-1-one)[1] have been described in the literature as inhibitors of chemoresistance (*14*), ovarian cancer cell proliferation (*15*), pulmonary carcinogenesis (*16*), proliferation of HGC-27 cells derived from human gastric cancer, and other tumorigenic effects (*17*). Licochalcone-A, a chalcone derivative found in the licorice root, has been associated with a wide variety of anticancer effects, along with other potential benefits (*18*). Chalcone synthesis is relatively straightforward using Claisen-Schmidt aldol condensation protocols, while the compounds themselves are susceptible to Michael addition at the ene-one (CH═CH−CO) moiety (*14*, *19*). These broad antitumor properties of chalcones prompted us to characterize these compounds at the molecular level for possible interactions with the p53/MDM2 system. Here, we describe NMR evidence for binding of chalcones in and near the tryptophan binding pocket of the p53 binding cleft of human MDM2 and propose three-dimensional models consistent with these data.

RESULTS AND DISCUSSION

Chalcones Are MDM2 Antagonists. Derivatives of the chalcone class have been shown to inhibit MDM2 binding to a p53 peptide in a two-site ELISA (Figure 1). The biotinylated optimized p53 peptide, which was coated to a Streptavidin-coated plate, was bound to MDM2 protein. Compounds interfering with the interaction were selected. Since only an 11-mer peptide was used in the ELISA carrying the MDM2 binding site, possible artifacts of

[†] Wojciech Zeslawski received a postdoctoral fellowship from the Humboldt Foundation. Raphael Stoll gratefully recognizes support from the Studienstiftung and the Fonds der Chemischen Industrie. This work was supported by DFG grants (SFB 413, 469).

* To whom correspondence should be addressed. E-mail: holak@biochem.mpg.de.

[‡] Max Planck Institute of Biochemistry.

[§] Roche Diagnostics GmbH.

[#] Tübingen University.

[1] Abbreviations: 2D and 3D, two- and three-dimensional; ppm, parts per million; NOE, nuclear Overhauser effect; NOESY, two-dimensional NOE spectroscopy; TOCSY, total correlation spectroscopy (homonuclear Hartmann−Hahn spectroscopy); CT, constant time; HSQC, heteronuclear single quantum coherence spectroscopy; ELISA, enzyme-linked immunosorbant assay; EMSA, electrophoretic gel mobility shift assay; chalcone, 1,3-diphenyl-2-propen-1-one.

10.1021/bi000930v CCC: $20.00
Published on Web 12/13/2000

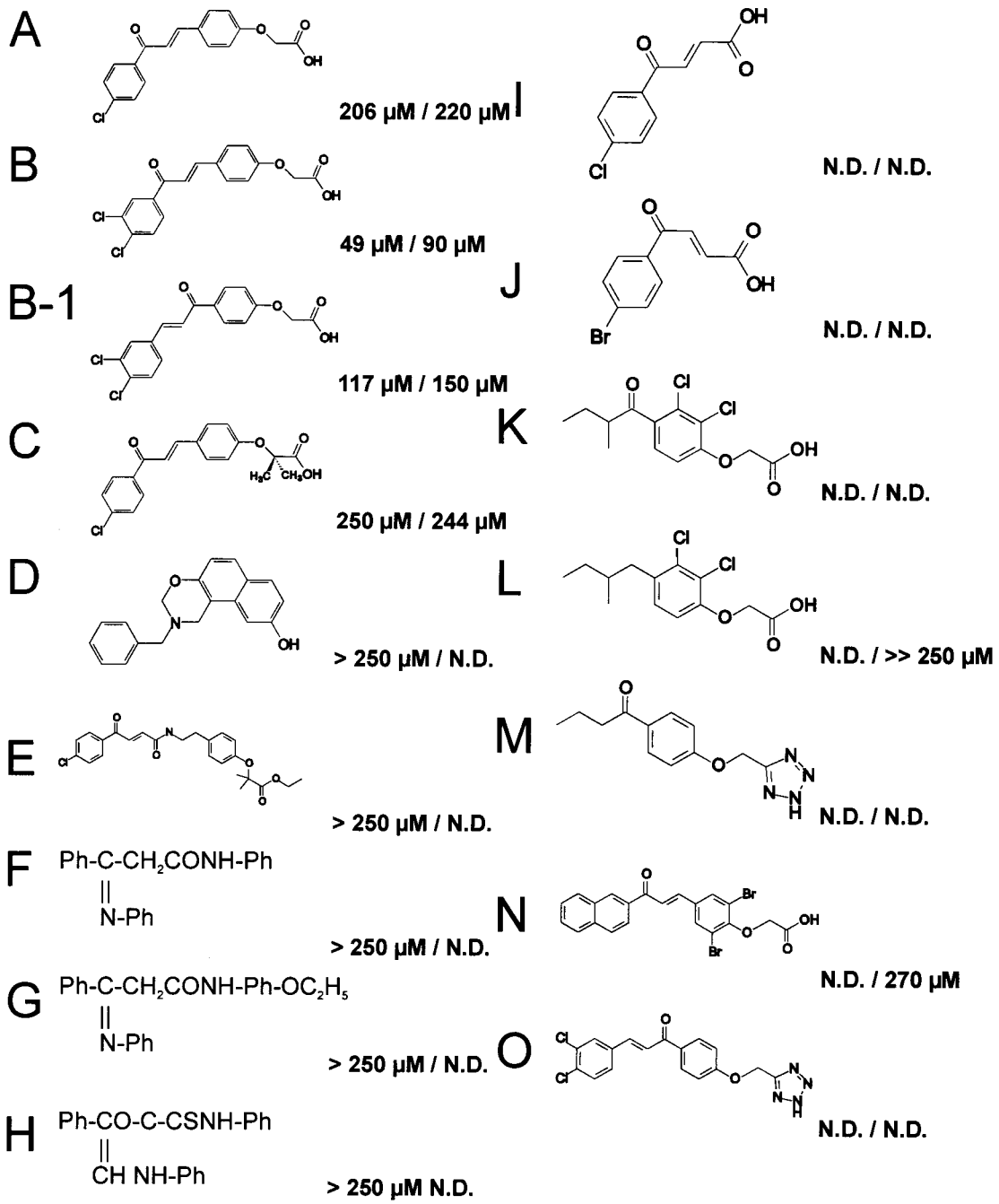

FIGURE 1: A representative collection of basic chalcone skeletons used in our study. Inhibition of MDM2 binding to p53 measured by ELISA (IC_{50} values given on the left side of the slash) and by NMR titration experiments (K_D values given on the right side of the slash). Compound D was studied as a negative control. For details refer to text.

secondary or allosteric binding sites are excluded. Because chalcones at certain concentrations induce precipitation/aggregation of MDM2, caution has to be exercised in interpreting the ELISA and EMSA data presented here. However, the ELISA data exhibited a range of IC_{50} values generating a rough structure−activity relationship profile. Compounds B, N, and O denature MDM2. Compound B-1 (Figure 1) leads to aggregation of the MDM2 but not of the human $p19^{INK4d}$ protein when applied in the same molar excess, as visualized by NMR. Induction of protein aggregation is usually considered as a nonspecific effect of compounds and therefore an indicator of low therapeutic potential. However, aggregation may either arise as a biochemical artifact or as a consequence of a specific interaction. In either case, the substance would inactivate the p53-specific interaction and lead to degradation of cellular MDM2.

Release of p53 Active for DNA Binding by Chalcones. Since the compounds were able to compete with MDM2 for binding to the p53 peptide as shown by ELISA, it was then tested whether they could dissociate preincubated p53/MDM2 complexes and release p53 active for DNA-binding in an electrophoretic gel mobility shift assay (EMSA). Here, full-length, tetrameric p53 protein was used instead of a short peptide. In this setting, the MDM2 protein supershifts p53 bound to its consensus DNA, confirming previously published data (*24*) (Figure 2). Since the compounds are dissolved in DMSO, incubation with 5% DMSO was shown

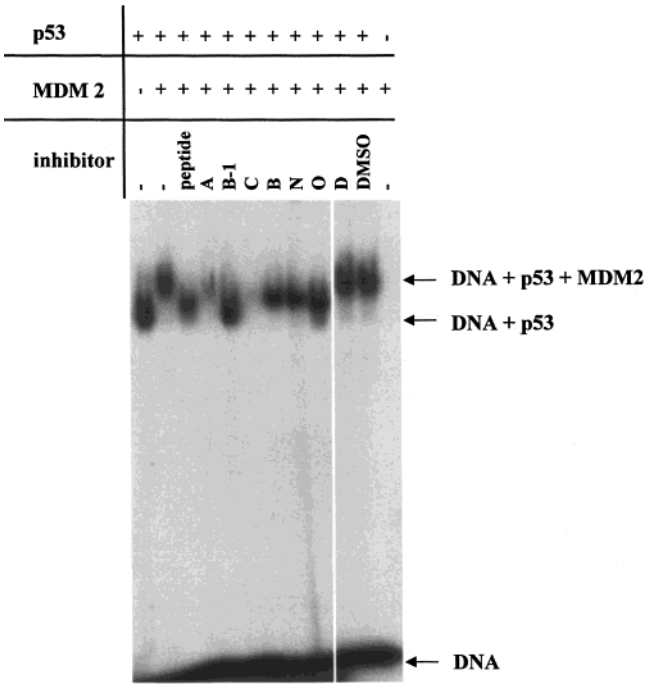

FIGURE 2: Effect of chalcones on DNA binding activity of p53/MDM2 complexes. Human p53 was analyzed for DNA binding following incubation with and without MDM2 using a electrophoretic gel mobility shift assay (EMSA). Preformed p53/MDM2 complexes were subjected to incubation with competing p53 peptide (250 μM) or low molecular weight compounds (1 mM). Since the compounds contained a final concentration of 5% DMSO, a DMSO control of 5% was included.

not to influence complex formation, as well as a control compound D (Figure 2). However, the binding of p53 and MDM2 was dissociated by addition of a p53 peptide containing the MDM2 binding site, which thus competes with p53 protein for binding to MDM2 (Figure 2).

Compounds A and C resolve the p53/MDM2 complex, however, without releasing active p53 (Figure 2). Thus, the compound interaction seems to additionally influence the p53 protein, which would not be anticipated from the ELISA. Compounds B, N, and O partially remove MDM2 from the complex with p53 by lowering the supershift. The released p53 still migrates higher than the p53 only control, which could indicate some molecules are MDM2 bound. Despite good IC_{50} values in the ELISA, the effect of the compound seems to be lower in the context of the full-length p53 protein complexed to MDM2. Compound B-1 completely resolves the supershift induced by MDM2 binding and releases active p53.

NMR Spectroscopy. Determination of binding sites of lead chalcone compounds were carried out using ^{15}N-HSQC NMR spectroscopy of the ^{15}N isotopically enriched domain of human MDM2 including residues 1−118. A nearly complete assignment of the backbone $^{1}H^{N}$ and ^{15}N NMR resonances was obtained for the uncomplexed MDM2 (apo-MDM2; Figure 3). The NMR ^{15}N-{^{1}H} NOE experiment indicated that the folded core of the MDM2 domain in solution extends from T26 to N111 (Figure 4). This is in good agreement with the crystal structures of N-terminal domains of human and Xenopus MDM2 in complex with a transactivation domain peptide of p53, where the MDM2 structure was also defined from T26 to V109 (*6*). The p53 peptide, comprising the residues 15 to 29, binds to an elongated hydrophobic cleft of the MDM2 domain. The interaction is primarily hydrophobic in character; only two hydrogen bonds are found between MDM2 and the p53 peptide. The hydrophobic surfaces of MDM2 and p53 are sterically complementary at the interface. The binding surface of p53 is dominated by a triad of p53 amino acids (F19, W23, and L26) that bind along the MDM2 cleft and define the corresponding phenylalanine, tryptophan, and leucine subpockets for the p53/MDM2 interaction (*6*) (Figure 6). In this classification, the leucine pocket is defined by Y100, T101, and V53, the tryptophan pocket is defined by S92, V93, L54, G58, Y60, V93, and F91, the phenylalanine pocket is defined by R65, Y67, E69, H73, I74, V75, M62, and V93 (*6*).

As a control experiment using a known stable MDM2/inhibitor complex, MDM2 was titrated with the p53 peptide comprising residues E17 to N29 (Figure 5, panel A, and Figure 6). NMR spectra showed that the p53 peptide/MDM2 complex was long-lived on the NMR chemical shift time scale (ref *20*; see also Materials and Methods). This is in agreement with the ELISA data that showed an apparent K_D of 0.6 μM (*6*). As can be seen in Figure 5, panel A, and Figure 6, panel B, almost all amino acids of the free MDM2 exhibit changes in chemical shifts upon complexation with the p53 peptide. The analysis of ligand-induced $^{1}H^{N}$ and the ^{15}N shifts was performed by applying the equation of Pythagoras to weighted chemical shifts which is in concordance with the recent literature (*21*). The largest shifts lined the three binding subpockets of p53 on MDM2 (Figure 5, panel A, and Figure 6, panel B). The full set of MDM2/p53 interface residues comprises M50, L54, L57, G58, I61, M62, Y67, H73, V75, F91, V93, H96, I99, and Y100 of MDM2 (*6*). Additionally, significant shifts are observed for β-strand residues T26, L27, V28, R29, L107, and V108 and for residues L34, L37, and K64 (Figure 5, panel A, and Figure 6, panel B). Shifts observed for amides outside the binding regions may be caused by secondary effects, such as allostery or change in mobility upon binding, and do not necessarily indicate direct binding of the p53 peptide to MDM2. Such possible secondary effects (e.g., residues L34, L37, and K64) must be considered when analyzing ligand binding to allosteric proteins.

All K_D values determined by NMR spectroscopy fully agree with the affinities measured by the ELISA binding assay (Figure 1). Compound A, with an ELISA IC_{50} value of 206 μM, shows the strongest shifts at the peptide groups of E52, V53, L54, F55, Y56, L57, G58, Y60, I61, and H73 (Figure 1, Figure 5, panel B, and Figure 7, panel A). Except for H73, all of these are found on the α-helix comprising residues M50-R65; we attribute the H73 shift to secondary or allosteric effects. The shift pattern is consistent with binding in the tryptophan pocket of MDM2. Compounds B and B-1 yielded similar chemical shift patterns as compared to compound A (Figure 5, panels B, C, and D). The shifts observed for compounds B and B-1 cannot reliably be used to localize the inhibitor interaction site because these inhibitors induce precipitating MDM2/MDM2 interactions that also contribute to the chemical shift pattern. The same is true for compounds N and O.

Chalcone C differs from A by the addition of two methyl groups near the acid terminus, an alteration that insignificantly affects the IC_{50} value (250 μM). The overall NMR shift perturbation pattern is similar to that observed for

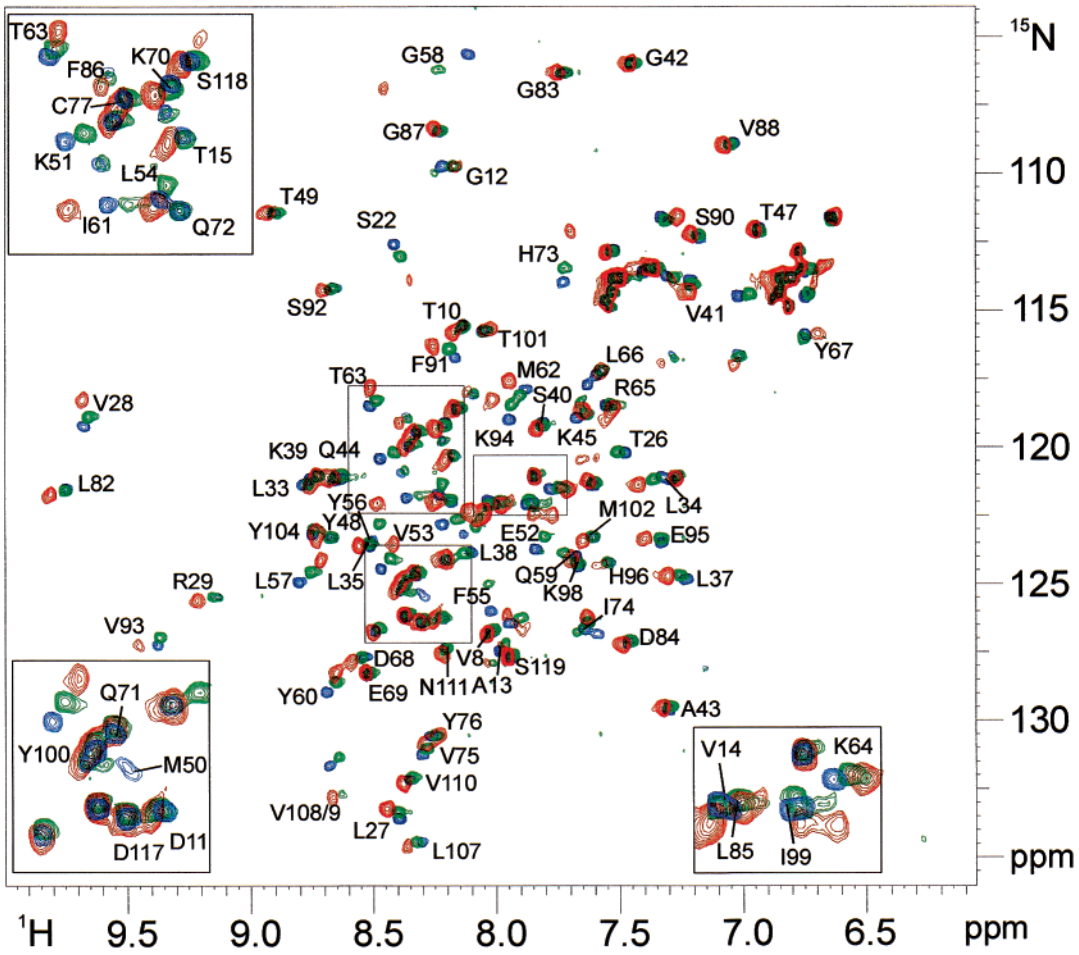

FIGURE 3: 500 MHz 2D ^{1}H-^{15}N HSQC spectrum of human MDM2 titrated with increasing amounts of chalcone C. Cross-peaks for apo-MDM2 are marked in blue; green and red cross-peaks indicate 50 and 100% complexation of MDM2 by chalcone C. Residue specific assignment of the backbone ^{1}H and ^{15}N frequencies is indicated.

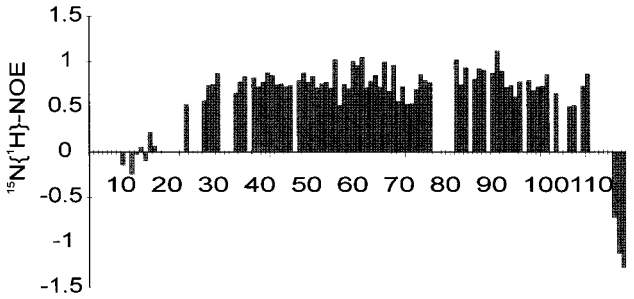

FIGURE 4: ^{15}N{^{1}H}-NOE for the backbone amides of human MDM2. Residues for which no results are shown correspond either to prolines or to residues where relaxation data could not be extracted.

chalcone A (Figures 1 and 3, Figure 5, panel E, and Figure 7, panel B). The detailed shift perturbation pattern, however, is changed by the dimethyl substitution: the perturbations observed for T26, K51, and E52 are new or greater, while the perturbations at Y56 and I61 caused by compound C are weakened (Figure 5, panels B and E, and Figure 7, panels A and B).

Hypothetical models for the binding modes may be generated using these data (Figures 7 and 8). First, a survey of chalcones from the Cambridge Database confirms the overall rigidity and planarity of the extended π-system. Thus, with the assumption described above that the monosubstituted phenyl group binds in the tryptophan pocket, a rotation of the rigid chalcone about the monochlorophenyl group would displace the perturbations from the "lower" region of helix M50−R65 toward the N-terminus to the "upper" region of the helix of the tryptophan subsite. This reflects the perturbation patterns of compound A (including I61 and Y56) and C (T26, K51, E52). Chalcones A and C, docked into the tryptophan subsite, are oriented with acid groups extended toward the solution; the chalcone carbonyl group is also solvent-exposed (Figure 8). The second phenyl group is also relatively solvent-exposed but encounters the similarly exposed F55 of MDM2 to join a cluster of aromats that further includes Y56. In addition, the acid group can be placed near the base of K51, which is found in a salt bridge interaction with E25 in the crystal structure (*6*). An intriguing hypothetical possibility is that a salt bridge is formed between K51 and the acid of compound C, with the two methyl groups in a hydrophobic interaction with the aliphatic portion of the lysine side chain. This would break the salt bridge with E25; a conformational change here could cause the amide shift perturbation at T26 as the amide proton is oriented to the same side of the β-sheet T26−P30. Without the two methyl groups of compound C to contribute to K51 binding and compete with E25 for salt bridge formation, compound A would be free to optimize the aromatic group interactions with F55, Y56, and the tryptophan pocket, leading to a binding conformation in the region and the greater number of perturbations observed for this compound (Figure 8).

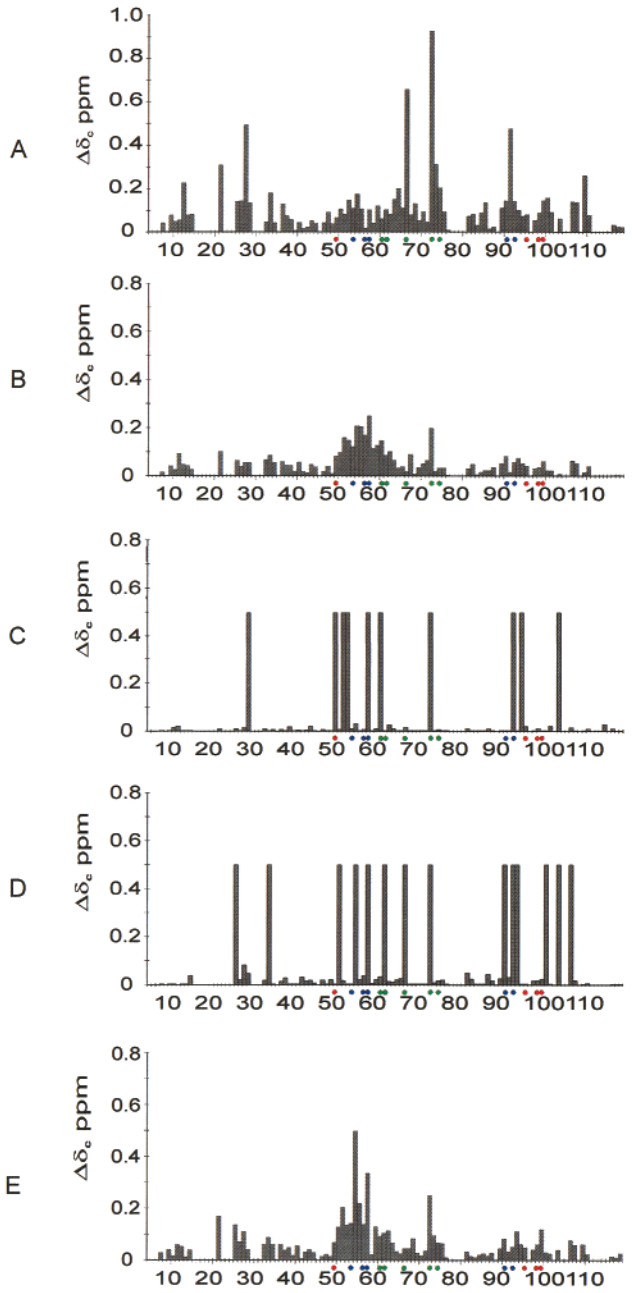

FIGURE 5: Plots of induced differences in the NMR chemical shifts versus the amino acid sequence. (A) The p53 peptide; (B) inhibitor A; (C) inhibitor B; (D) inhibitor B-1 (for the maximum induced shifts for B and B-1 see explanation in experimental procedures); (E) inhibitor C. Red, blue, and green dots mark the leucin-, tryptophan-, and the phenylalanine-binding site on human MDM2 (refer to Figure 6).

Other non-main chain amide (Gln, Asn) shifts are observable in the spectra and can in principle contribute additional information. One such side chain is Q72 that is bound to the p53 peptide in the crystal structure (*6*). If the outlying amide shift at H73 observed in our experiments is caused by direct ligand binding interactions, the amide of the adjacent side chain Q72 might shift as well. However, for all derivatives of chalcones used in this study, we did not observe any prominent shifts for the side chain protons H_ϵ of Q72. This is further corroborative evidence for the binding site of A and C in the tryptophan pocket and distant from Q72−H73. Therefore, we conclude that the shifts observed for H73 are secondary and may be caused by changes in the protonation state of the solvent-exposed imidazole ring as the pH of 7.4 the sample was close to the pK_s of the histidine side chain. Another hypothetical explanation for the shifts of H73 observed upon binding of chalcone derivatives is sensitivity to χ-rotamer transitions.

In conclusion, we have shown that chalcone derivatives bind to the tryptophan pocket of the p53 binding site of MDM2 and are able to dissociate the p53/MDM2 complexes. Therefore chalcones, as antagonists of the p53/MDM2 interaction, offer the starting point for structure-based drug design for cancer therapeutics in strategies that abolish constitutive inhibition of p53 in tumors with elevated levels of MDM2 or, more generally, in strategies that enhance p53 activity.

MATERIAL AND METHODS

Protein Expression and Purification. The recombinant human MDM2 protein was obtained from an *Escherichia coli* BL21(DE3) expression system and contained the first 118 N-terminal residues of human MDM2 cloned in a pQE-40 vector (Qiagen), C-terminally extended by an additional serine residue. The protein was renatured from *E. coli* inclusion bodies as previously published (*25*). Refolded MDM2 was applied first to a butyl Sepharose 4 Fast Flow (Pharmacia) and then to a HiLoad 16/60 Superdex75 gelfiltration column (Pharmacia). The uniformly $^{13}C/^{15}N$, and ^{15}N isotopically enriched protein samples were prepared by growing the bacteria in minimal media containing $^{15}NH_4Cl$ either with or without $^{13}C_6$-glucose. For selectively enriched samples (^{15}N-Val, ^{15}N-Leu, and ^{15}N-Phe), the minimal medium consisted of 300−1000 mg L^{-1} of the isotopically enriched amino acids and all other amino acids (*26*, *27*). A reverse ^{14}N-His sample of human MDM2 was prepared by adding 300−1000 mg L^{-1} of ^{14}N-His to the minimal medium containing $^{15}NH_4Cl$ (*26*). The p53 peptide comprising residues E17 to N29 of human p53 was chemically synthesized and contained an additional cysteine at the N-terminus. The peptide was purified by reversed phase chromatography.

p53/MDM2 Binding ELISA. Interference of the p53/MDM2 binding by low molecular weight compounds was measured in a 96-well polypropylene round-bottom microtiter plate (Costar, Serocluster). Human MDM2 (amino acids 1−118, at 40 nM) was preincubated with PBS/0.05% Tween50 (PBST)/10% DMSO or low molecular weight compounds. After 15-min incubation of the sample, 100 nM of a p53-derived peptide (MPRFMDYWEDL, biotinylated, synthesized on solid phase) was added (*39*). As a negative control, buffer only was added into separate wells (blanks). After another 30 min, the incubation mixture was added to 96-well plates coated with streptavidin. After 1 h, the wells were extensively washed with PBS/0.05% Tween50. Then, the MDM2 specific antibody (N20, Santa Cruz Biotechnology) in PBST and 1% casein was added. After 1 h, the wells were thoroughly washed with PBST and the secondary antibody (anti-rabbit-IgG-POD, RMB) in PBST and 1% casein was added. After another hour, the wells were washed with PBST, and the peroxidase subtrate ABTS was added. After 30 min, OD405/490 nm was determined with a Dynatech MR 7000 ELISA reader. Calculation of inhibition was done as follows: [1 − (OD405/490 nm compounds − OD405/490 nm blanks)/(OD405/490 nm 100% values −

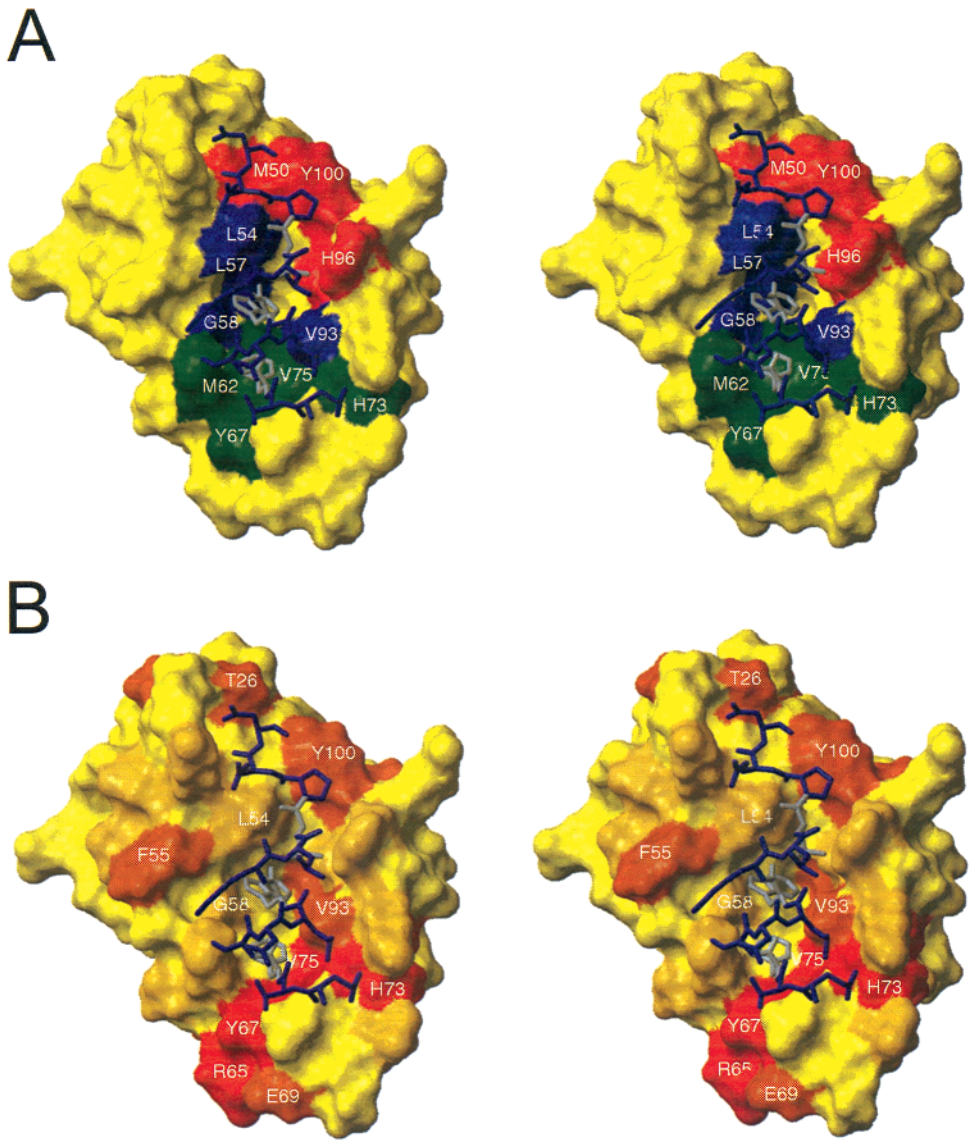

FIGURE 6: (A) Contact surface of human MDM2 (residues 25−109) generated with MOLMOL from the 1YCR data set (*6*, *38*). The atom radius was set to the van der Waals value and the solvent radius to 1.4 Å. The p53 peptide is superimposed in blue sticks as a reference with side chain residues of F19, W23, and L26 colored in light blue. Residues of human MDM2 that constitute the leucin-, tryptophan-, and the phenylalanine-binding are colored in red, blue, and green, respectively. (B) Contact surface of human MDM2 as in panel A. Residues that show significant induced NMR chemical shifts upon complexation with the p53 peptide are highlighted. These residues are shown in yellow, orange, light red, and dark red for observed vectorial shifts smaller than 0.08, 0.08−0.12, and 0.12−0.2 ppm and greater than 0.2 ppm, respectively. The p53 peptide is superimposed in blue sticks as a reference with side chain residues of F19, W23, and L26 colored in light blue.

OD405/490 nm blanks)] × 100 = % inhibition. Compounds were titrated to determine IC_{50} values twice (range of compound concentration: 0.5, 1, 5, 10, 25, 50, 125, 250 μM).

Gel Shift Assays. The DNA binding assay was performed using active fractions of human p53 protein expressed in baculovirus-infected insect cells and purified on Hi-Trap Heparin-Sepharose (Pharmacia Biotech) in a linear gradient from 0.1 to 0.85 M KCl (*22*). MDM2 containing the first 118 amino acids was cloned as a GFP (green fluorescent protein) fusion protein at its N-terminus, which served to enlarge the protein to obtain a significant shift in the electrophoretic gel mobility shift assay (EMSA). (Larger fragments of the MDM2 protein tended to aggregate and were therefore not used.) Additionally, MDM2 was His-tagged C-terminally by $(His)_6$, which were added via a linker segment containing (Ser−Arg−Gly−Ser) for convenient purification. The construct was cloned in a modified pQE-40 vector (Qiagen) and expressed in *E. coli* BL21 (DE3) at 22 °C as soluble protein. The lysate was purified using a Talon column (Clontech) according to standard protocols. p53 was bound to its specific, double-stranded DNA consensus site (PG) (*23*), which was labeled with [γ-^{32}P]-ATP. To ensure sequence-specific binding, a 20-fold (200 ng) excess of nonlabeled supercoiled competitor DNA (pBluescript II SK+, Stratagene) was included. p53 protein was used at a concentration of 200 nM and MDM2 at 2 μM. Despite the apparent excess of the proteins over the used DNA, the active fraction of the total protein preparation is so small that the DNA is still in excess, as can also be seen from the free DNA in Figure 2. The p53 peptide was used at 250 μM, compounds at 1 mM. p53 was preincubated with MDM2 at RT for 30 min prior to addition of compounds for 30 min at 4 °C and, finally, addition of DNA in DNA binding buffer for another 15 min at 4 °C. The DNA binding

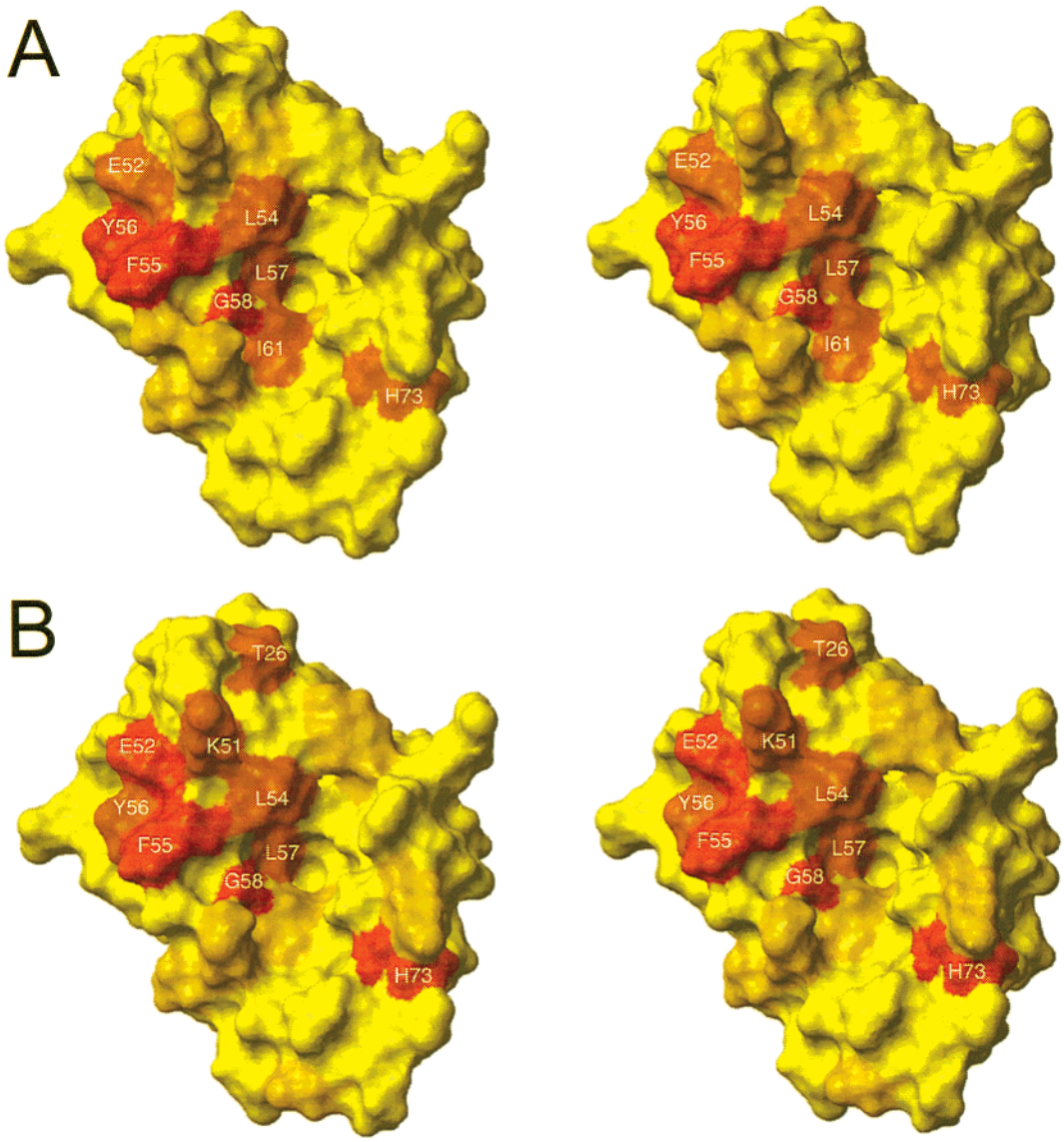

FIGURE 7: Residues that show significant induced NMR chemical shifts upon complexation with chalcone derivatives. These residues are shown in yellow, orange, light red, and dark red for observed vectorial shifts smaller than 0.08, 0.08−0.12, and 0.12−0.2 ppm, and greater than 0.2 ppm, respectively. Contact surface of human MDM2 (residues 25−109) generated with MOLMOL from the 1YCR data set (*6*, *38*). The atom radius was set to the van der Waals value and the solvent radius was set to 1.4 Å. No shift perturbations greater than 0.08 ppm were observed for residues located on the backside of MDM2 for compounds in panels A and B. (A) Chalcone A; (B) chalcone C.

buffer contained: 20% (v/v) glycerol, 50 mM KCl, 40 mM Hepes, pH 8, 5 mM DTT, 0.1% Triton X-100, 10 mM $MgCl_2$, 1.0 mg mL^{-1} bovine serum albumin. The reaction mix was loaded onto a 4% native polyacrylamide gel and separated at 200 V for 2 h at 4 °C. The gel was dried and the DNA was detected by autoradiography.

NMR Spectra and Assignments. All NMR spectra were acquired at 290 and 300 K on Bruker AMX500, DRX500, DRX600, and DMX750 spectrometers. Typically, NMR samples contained up to 0.5 mM of protein in 50 mM KH_2PO_4, 50 mM Na_2HPO_4, 150 mM NaCl, pH 7.4, 5 mM DTT, 0.02% NaN_3, and protease inhibitors. The quality of the spectra for MDM2 with and without inhibitors was reduced by aggregation, especially at concentrations higher than 0.5 mM at pH 7.4 and 300 K. Since concentrated samples remained stable for approximately 1 day, only highly sensitive experiments could be performed. A nearly complete assignment of the backbone $^1H^N$ and ^{15}N NMR resonances was obtained for the uncomplexed MDM2 (apo-MDM2; Figure 3). Backbone sequential resonances were assigned with CT-HNCA, CBCA(CO)NH using the WATERGATE sequence, and in part with 2D TOCSY (mixing time of 42 ms), 2D NOESY (mixing time 120 ms), 3D ^{15}N-TOCSY-HSQC (spin-lock period of 36 ms), and 3D ^{15}N-NOESY-HSQC (mixing time of 120 ms) experiments (*28*−*33*), and by selective enrichment using ^{15}N-Leu, Phe, Val, and reverse ^{14}N-His samples of MDM2. ^{15}N-{^1H} heteronuclear NOE was measured using a modified version of the experiments as described previously (*34*, *35*). NOE values were calculated by scaling ratios of peak heights in the NOE experiment with ^1H presaturation and the standard HSQC experiment obtained from the same sample. Recording of the NOE experiment without proton saturation using the same sample was not possible due to the fast precipitation of apo-MDM2 samples. This simplified approach introduces an additional error of approximately 10−20% to the NOE values. The experiment

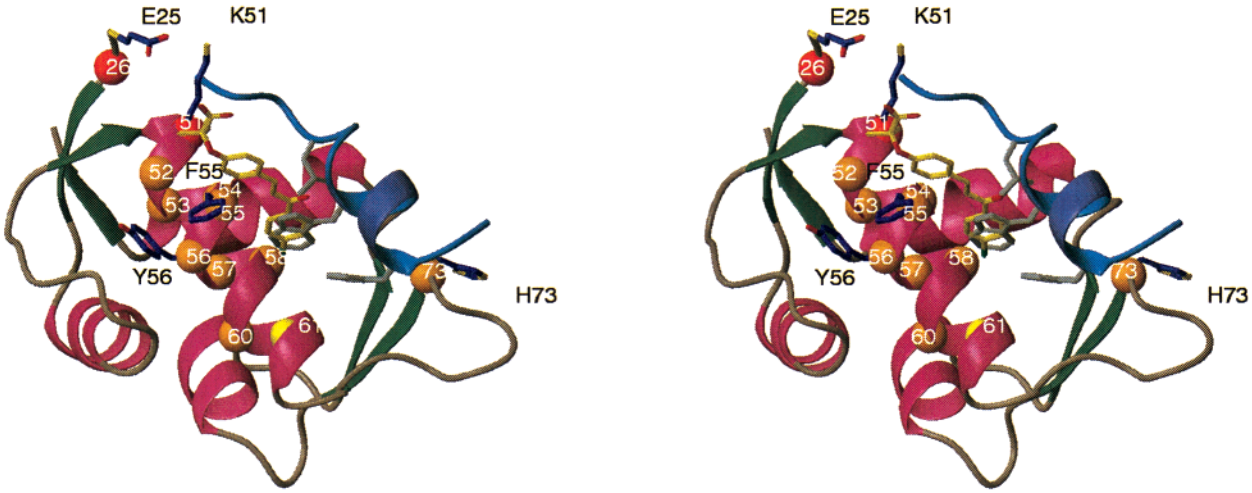

FIGURE 8: Model of human MDM2 in complex with chalcone C (shown in yellow sticks) superimposed with the p53 peptide (shown in blue). The colored spheres indicate residues that showed significant induced chemical shifts upon complexation with the chalcone. For details refer to text.

was recorded in an interleaved manner so that precipitation of the protein results in broadening of the signals but does not affect the extracted NOE values (*34*).

Ligand Binding. All chalcone derivatives used in this study have been synthesized according to standard Claisen−Schmidt aldol condensation protocols as previously published (*14*, *19*). A total of 50 chalcone derivatives were synthesized. NMR measurements consisted of monitoring changes in chemical shifts and line widths of the backbone amide resonances of uniformly ^{15}N-enriched MDM2 samples (*36*, *37*) in a series of HSQC spectra as a function of a ligand concentration (*36*). No changes in chemical shifts were observed between samples of different concentrations (0.03−0.5 mM) and pH values between 6.5 and 7.5. For titration experiments, 0.1−0.3 mM of human MDM2 in 50 mM KH_2PO_4, 50 mM Na_2HPO_4, 150 mM NaCl, pH 7.4, and 5 mM DTT was used. The chalcone derivatives were lyophilized and finally dissolved in DMSO-d_6. No shifts were observed in the presence of 1% DMSO (the maximum concentration of DMSO in all NMR experiments after addition of inhibitors). All chalcone−MDM2 complexes showed a continuous movement of several NMR peaks upon addition of increasing amounts of inhibitors. From these experiments, the spectra of MDM2 could be assigned unambiguously. The complexes of human MDM2 and the chalcones were prepared by mixing the protein and the ligand in the NMR tube. Typically, NMR spectra were recorded 15 min after mixing at room temperature. An initial screening of all compounds used in this study was performed with a 10-fold molar excess of chalcone to human MDM2. All subsequent titrations were carried out until no further shifts were observed in the spectra. Saturating conditions were achieved at a molar ratio of chalcone to MDM2 of 6 for chalcone A, of 2 for chalcone B, of 2 for chalcone B-1, and of 6 for chalcone C, for example. Typically, the concentration of human MDM2 was 0.1 mM and the final concentration of the chalcone ligand was 50 mM in each titration. All K_D values obtained by NMR spectroscopy are based on at least six data points. From the independently determined IC_{50} values and the K_D constants, one ligand binding site for these chalcones per MDM2 is calculated taking into account the molar ratio of ligand to protein in the NMR experiments. Quantitative analysis of induced chemical shifts were performed on the basis of spectra obtained at saturating conditions of each chalcone. Analysis of ligand-induced shifts was performed by applying the equation of Pythagoras to weighted chemical shifts: $\Delta\delta_c(^1H, ^{15}N) = [\{|\Delta\delta(^1H)|^2 + 0.2 \times |\Delta\delta(^{15}N)|^2\}^{0.5}]$. The p53 peptide/MDM2 complex was long-lived on the NMR chemical shift time scale (lifetimes $\gg$ 2 ms) (*20*). Two separate sets of resonances were observed in the ^{1}H-^{15}N HSQC spectra, one corresponding to free MDM2 and the other to MDM2 bound to the p53 peptide. For well-resolved, isolated peaks, the assignment of Figure 3 could be transferred to the resonances in the peptide complex (54% of all backbone amide resonances in the ^{1}H-^{15}N HSQC). For the rest of the shifts, assignment of $\Delta\delta_c(^1H, ^{15}N)$ upon complex formation was carried out in a conservative manner, i.e., for these shifts the distance in ppm to the closest peak in complexed MDM2 was chosen. In addition, all selectively enriched samples of human MDM2 (^{15}N-Val, ^{15}N-Leu, ^{15}N-Phe, and reverse ^{14}N-His) were titrated with the p53 peptide to confirm a subset of MDM2/p53 complex assignments. Only $\Delta\delta_c(^1H, ^{15}N)$ values larger than 0.1 ppm were considered to be significant. $\Delta\delta_c(^1H, ^{15}N)$ smaller than 0.1 ppm were found for 37 residues. Erroneous conclusions could result if some of the residues with $\Delta\delta_c(^1H, ^{15}N) < 0.1$ ppm were actually in contact with the inhibitor. However, the internal consistency of our results corroborates our analysis; for example, no core buried residue was found that had $\Delta\delta_c(^1H, ^{15}N) > 0.1$ ppm. Furthermore, all residues of human MDM2 involved in binding to the p53 peptide also show significant shifts $\Delta\delta_c(^1H, ^{15}N)$ upon complexation with the peptide (*6*). For compounds B and B-1 (Figure 5, panels C and D), the maximum shifts shown at $\Delta\delta_c = 0.5$ ppm correspond to the cross-peaks of the folded core of MDM2 whose line-widths broaden 2-fold upon addition of either B or B-1 in the molar ratio of B-1 to MDM2 1:1 and disappear thereafter at the titration ratio 2:1 (*37*). Compound D (Figure 1) was studied as a negative control because it did not inhibit MDM2 binding to a p53 peptide as measured by ELISA. This compound does not bind to apo-MDM2, as no ^{1}H and ^{15}N shifts greater than 0.1 ppm were observed in the NMR spectra. As this compound was available in our laboratory and because of its similar size as compared to the chalcone

skeleton, we have selected this heterocyclic system as a negative control for any organic compound. Other negative control NMR titration experiments included the chemically synthesized chromophore of the green fluorescent protein as well as a synthetic 22-residue peptide. None of the control ligands led to significant chemical shift pertubations (data not shown). Chalcone B-1 generally enhances the intrinsic tendency of MDM2 to aggregate at higher concentrations. Therefore, an additional experiment was performed to test their specificity and to rule out a property as a general protein precipitant. For this purpose, the human tumor suppressor $p19^{INK4d}$ was purified as previously described (*40*). Chalcone B-1 did not induce aggregation of $p19^{INK4d}$ when applied under the same experimental conditions.

ACKNOWLEDGMENT

We thank Roberto Di Domenico and Ernesto Menta for providing the low molecular weight compounds and Rosa-Maria Busl-Schuller and Lorenz Perras for excellent technical support.

REFERENCES

1. Juven-Gershon, T., and Oren, M. (1999) *Mol. Med. (N. Y.) 5*, 71−83.
2. Momand, J., Jung, D., Wilczynski, S., and Niland, J. (1998) *Nucleic Acids Res. 26*, 3453−3459.
3. Lane, D. P., and Hall, P. A. (1997) *Trends Biochem. Sci. 22*, 372−374.
4. Oliner, J. D., Kinzler, K. W., Meltzer, P. S., George, D. L., and Vogelstein, B. (1992) *Nature 358*, 80−83.
5. Lozano, G., and Montes de Oca Luna, R. (1998) *Biochim. Biophys. Acta 1377*, M55−M59.
6. Kussie, P. H., Gorina, S., Marechal, V., Elenbaas, B., Moreau, J., Levine, A. J., and Pavletich, N. P. (1996) *Science 274*, 948−953.
7. Oliner, J. D., Pietenpol, J. A., Thiagalingam, S., Gyuris, J., Kinzler, K. W., and Vogelstein, B. (1993) *Nature 362*, 857−860.
8. Haupt, Y., Maya, R., Kazaz, A., and Oren, M. (1997) *Nature 387*, 296−299.
9. Kubbutat, M. H. G., Jones, S. N., and Vousden, K. H. (1997) *Nature 387*, 299−303.
10. Momand, J., Zambetti, G. P., Olson, D. C., George, D., and Levine, A. J. (1992) *Cell 69*, 1237−1245.
11. Midgley, C. A., and Lane, D. P. (1997) *Oncogene 15*, 1179−1189.
12. Chen, J., Marechal, V., and Levine, A. J. (1993) *Mol. Cell. Biol. 13*, 4107−4114.
13. Wasylyk, C., Salvi, R., Argentini, M., Dureuil, C., Delumeau., I., Abecassis, J., Debusche, L., and Wasylyk, B. (1999) *Oncogene 18*, 1921−1934.
14. Daskiewicz, J. B., Comte, G., Barron, D., Di Petro, A., and Thomasson, F. (1999) *Tetrahedron Lett. 40*, 7095−7098.
15. Devincenzo, R., Scambia, G., Panici, P. B., Ranelletti, F. O., Bonanno, G., Ercoli, A., Dellemonache, F., Ferrari, F., Piantelli, M., and Mancuso, S. (1995) *Anti-Cancer Drug Des. 10*, 481−490.
16. Wattenberg, L. (1995) *J. Cell. Biochem. Suppl. 22*, 162−168.
17. Shibata, S. (1994) Shibata Lab. Nat. Med. Mater., Minophagen Pharm. Co., Tokyo, Japan, Stem Cells (Dayton), 12(1), 44−52.
18. Park, E. J., Park, H. R.; Lee, J. S., and Kim, J. (1998) *Planta Med. 64*, 464−466.
19. Bois, F., Boumendjel, A., Mariotte, A. M., Conseil, G., and Di Petro, A. (1999) *Bioorg. Med. Chem. 7*, 2691−2695.
20. Wüthrich, K. (1986) *NMR of Proteins and Nucleic Acids*. John Wiley & Sons, New York, Chichester, Brisbane, Toronto, Singapore.
21. Pellechia, M., Sebbel, P., Hermanns, U., Wüthrich, K., and Glockshuber, R. (1999) *Nat. Struct. Biol. 6*, 336−339.
22. Hansen, S., Hupp, T. R., and Lane, D. P. (1996) *J. Biol. Chem. 271*, 3917−3924.
23. El-Deiry, W., Kern, S. E., Pietenpol, J. A., Kinzler, K. W., and Vogelstein, B. (1992) *Nat. Genet. 1*, 45−49.
24. Böttger, A., Böttger, V., Garcia-Echeverria, C., Chene, P., Hochkeppel, H.-K., Sampson, W., Ang, K., Howard, S., Picksley, S. M., and Lane, D. P. (1997) *J. Mol. Biol. 269*, 744−756.
25. Jaenicke, R., and Rudolph, R. (1986) *Methods Enzymol. 131*, 218−50.
26. Kalus, W., Zweckstetter, M., Renner, C., Sanchez, Y., Georgescu, J., Grol, M., Demuth, D., Schumacher, R., Dony, C., Lang, K., and Holak, T. A. (1998) *EMBO J. 17*, 6558−6572.
27. Mühlhahn, P., Zweckstetter, M., Georgescu, J., Ciosto, C., Renner, C., Lanzendörfer, M., Lang, K., Ambrosius, D., Baier, M., Kurth, R., and Holak, T. A. (1998) *Nat. Struct. Biol. 5*, 682−686.
28. Grzesiek, S., and Bax, A.(1992) *J. Am. Chem. Soc. 114*, 6291−6293.
29. Grzesiek, S., and Bax, A. (1992) *J. Magn. Reson. 96*, 432−440.
30. Sklenář, V., Piotto, M., Leppik, R., and Saudek, V. (1993) *J. Magn. Reson. A 102*, 241−245.
31. Marion, D., Driscoll, P. C., Kay, L. E., Wingfield, P. T., Bax, A., Gronenborn, A. M., and Clore, G. M. (1989) *Biochemistry 28*, 6150−6156.
32. Jahnke, W., Baur, M., Gemmecker, G., and Kessler, H. (1995) *J. Magn. Reson. B 106*, 86−88.
33. Mori, S., Abeygunawardana, C., Johnson, M. N., and van Zijl, P. C. M. (1995) *J. Magn. Reson. B 108*, 94−98.
34. Farrow, N. A., Muhandiram, R., Singer, A. U., Pascal, S. M., Kay, C. M., Gish, G., Shoelson, S. E., Pawson, T., Foreman-Kay, J. D., and Kay, L. E. (1994) *Biochemistry 33*, 5984−6003.
35. Mühlhahn, P., Bernhagen, J., Czisch, M., Georgescu, J., Renner, C., Ross, A., Bucala, R., and Holak, T. A. (1996) *Protein Sci. 5*, 2095−2103.
36. Shuker, S. B., Hajduk, P. J., Meadows, R. P., and Fesik, S. W. (1996) *Science 274*, 1531−1534.
37. McAlister, M. S. B., Mott, H. R., van der Merwe, A., Campbell, I. D., Davis, S. J., and Driscoll, P. C. (1996) *Biochemistry 35*, 5982−5991.
38. Koradi, R., Billeter, M., and Wüthrich, K. (1996) *J. Mol. Graph. 14*, 51−55.
39. Böttger, V., Böttger, A., Howard, S. F., Picksley, S. M., Chène, P., Garcia-Echeverria, C., Hochkeppel, H.-K., and Lane, D. P. (1996) *Oncogene 13*, 2141−2147.
40. Baumgartner, R., Fernandez-Catalan, C., Winoto, A., Huber, R., Engh, R., and Holak, T. A. (1998) *Structure 6*, 1279−1290.

BI000930V